Published in final edited form as:

Curr Biol. 2023 June 19; 33(12): 2574–2581.e3. doi:10.1016/j.cub.2023.05.039.

Dynamic BMP signaling mediates notochord segmentation in zebrafish

Brianna Peskin[1], **James Norman**[1], **Jennifer Bagwell**[1], **Adam Lin**[1], **Priyom Adhyapok**[1], **Stefano Di Talia**[1,2], **Michel Bagnat**[1,*]

[1]Department of Cell Biology, Duke University School of Medicine, Durham, NC27710, USA.

[2]Department of Orthopaedic Surgery, Duke University School of Medicine, Durham, NC27710, USA.

Summary

The vertebrate spine is a metameric structure composed of alternating vertebral bodies (centra) and intervertebral discs[1]. Recent studies in zebrafish have shown that the epithelial sheath surrounding the notochord differentiates into alternating cartilage-like (*col2a1*/*col9a2+*) and mineralizing (*entpd5a+)* segments which serve as a blueprint for centra formation[2–5]. This process also defines the trajectories of migrating sclerotomal cells that form the mature vertebral bodies[4]. Previous work demonstrated that notochord segmentation is typically sequential and involves the segmented activation of Notch signaling[2]. However, it is unclear how Notch is activated in an alternating and sequential fashion. Furthermore, the molecular components that define segment size, regulate segment growth, and produce sharp segment boundaries have not been identified. In this study, we uncover that a BMP signaling wave acts upstream of Notch during zebrafish notochord segmentation. Using genetically encoded reporters of BMP activity and signaling pathway components, we show that BMP signaling is dynamic as axial patterning progresses, leading to the sequential formation of mineralizing domains in the notochord sheath. Genetic manipulations reveal that type I BMP receptor activation is sufficient to ectopically trigger Notch signaling. Moreover, loss of Bmpr1ba and Bmpr1aa or Bmp3 function disrupts ordered segment formation and growth, which is recapitulated by notochord-specific overexpression of the BMP antagonist, Noggin3. Our data suggest that BMP signaling in the notochord sheath precedes Notch activation and instructs segment growth, facilitating proper spine morphogenesis.

Graphical Abstract

*Correspondence: michel.bagnat@duke.edu.

Author contributions

B.P and M.B conceived the study and wrote the manuscript with input from co-authors. B.P., J.N, J.B., and A.L. performed experiments. B.P, P.A., S.D., and M.B. analyzed data.

Declaration of interests

The authors declare no competing interests.

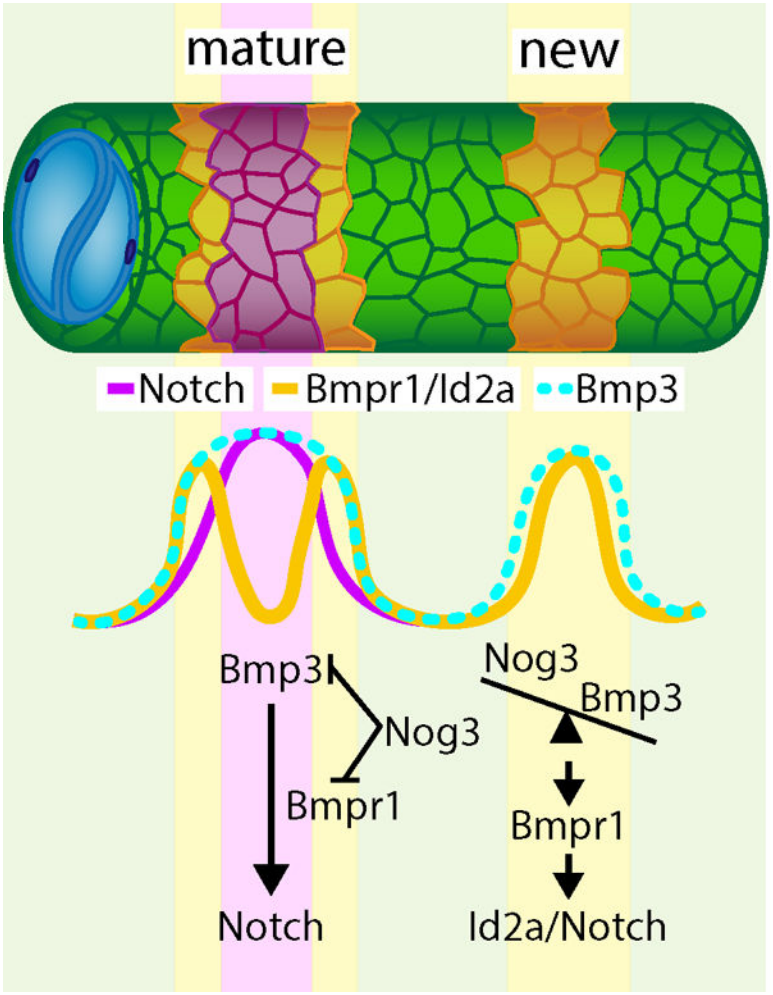

Results and Discussion

In zebrafish, the outer epithelial layer of the notochord sheath initially expresses *col2a1a* and *col9a2* (*col9a2*+ henceforth) uniformly. Around 5 days post-fertilization (dpf), alternating domains of sheath cells differentiate into *entpd5a+* cells sequentially along the anterior-posterior (AP) axis[2,3]. This process requires Notch activity[2] and induces a mineralization program[5] that forms rings of chordacentra around the *entpd5a+* domains to which osteoblast precursors are then recruited to form vertebral centra. Cells that continue to express *col9a2* are confined to the prospective intervertebral discs (IVDs)[2–4]. Sequential and segmented activation of Notch in precise regions along the notochord sheath is, therefore, crucial to establish properly spaced centra[2]. However, Notch activates simultaneously with *entpd5a,* suggesting it is a late marker of notochord segmentation. To identify upstream activators of Notch during notochord segmentation, we turned to RNA sequencing (RNAseq) data we previously generated from three populations of purified sheath cells (*col9a2+*, *entpd5a+*, and double+) at 13dpf[2]. Reviewing the RNAseq data, we identified several differentially expressed BMP signaling components (Figures 1A and S1A). BMPs are known to regulate cartilage and bone growth during development, and repair[6,7]. In mice, knockout of type

I BMP receptors leads to irregular chondrogenesis and endochondral ossification[8] and centra formation is disrupted in *Bmpr1b*$^{-/-}$ mice in which *Acvr1*, another BMP receptor, is conditionally knocked out from *Col2* expressing cells[9]. This suggests a role for BMPs in centra ossification. Moreover, in zebrafish, overexpression of Bmp2b induces hyperossification[10]. However, whether BMP signaling plays a role in establishing the location of centra domains or in the relative timing of centra formation along the AP axis is unknown.

Dynamic activation of BMP signaling during notochord segmentation

To investigate the role of BMP signaling during notochord segmentation, we first imaged a previously generated BMP activity reporter, *BRE:d2GFP*[11]. This reporter contains Smad 1/5 binding sites (BMP Responsive Elements) upstream of a minimal promoter and destabilized green fluorescent protein (d2GFP). Live confocal imaging revealed that *BRE:d2GFP* expression is highly dynamic in the notochord sheath as segmentation progresses (Figure 1B). To analyze the temporal dynamics of BMP signaling, we imaged 9 dpf larvae co-expressing *entpd5a:pkred* every 24 hours for 4 days (Figure 1C). Tracking individual cells, we found that sheath cells activate BMP signaling prior to expressing *entpd5a* (Figure 1C, yellow arrows). Once cells begin to express *entpd5a*, *BRE:d2GFP* expression decreases (Figure 1C cyan arrows). This generates a pattern of d2GFP fluorescence that peaks in the center of newly formed segments (Figure 1B brackets, 1D,D'), while in more mature segments expression is enriched on the edges of *entpd5a*+ domains (Figure 1B arrows, 1E,E'). Thus, BMP signaling is active at the center of newly differentiating segments and activity travels outward within each segment as mineralizing domains expand laterally.

Next, we examined the expression of *id2a,* a target of BMP signaling. Inhibitors of differentiation/DNA binding (ID) proteins are basic helix-loop-helix proteins that are direct, early targets of BMP 2/4 signaling[7,12]. Additionally, ID proteins are known to regulate Notch pathway activity in various tissues[13,14]. We found that the expression pattern of *id2a:GFPCaax, a* transgene we previously established[2], closely mirrors that of the BMP reporter (Figure 1F, F', and S1B). Together, these data show that BMP signaling is dynamic during sheath cell differentiation prior to *entpd5a* expression.

Bmp3 signaling precedes *entpd5a* activation and is required to specify the mineralizing cell fate

The *BRE:d2GFP* reporter contains binding sites for only Smads 1 and 5[11]. To obtain a more complete picture of BMP signaling in the notochord, we searched for additional BMPs in our RNAseq data and identified *bmp3* as the most highly expressed BMP ligand in sheath cells. *bmp3* is enriched in double+ cells (Figure 1A and S1A), corresponding to the newly differentiated mineralizing population. Bmp3, is a unique member of the BMP signaling family that is thought to oppose the osteogenic activity of canonical BMP (Bmp2/4) signaling in some contexts[15,16]. During endochondral ossification in mice, knockout of *Bmp3* can lead to increased ossification in trabecular bone[15,17]. However, overexpression of *Bmp3* has also been shown to increase the region of hypertrophic chondrocytes in mice[18], which share similarities with *entpd5a+* notochord sheath cells such as expression of collagen

type X, *mmp13a/b*, and *runx2b*[2,19]. These conflicting data from mice suggest that the role of BMP3 in ossification may be context dependent, making it difficult to predict how Bmp3 may function during notochord segmentation.

Bmp3 is known to activate Smads 2 and 3[20], which would not be detected by the *BRE:d2GFP* reporter. To visualize *bmp3* expression dynamics during notochord segmentation, we adapted a promoter knock-in method from previous work[21] to insert a destabilized fluorescent protein (VenusPest) into the *bmp3* locus. Fluorescence intensity analysis of *bmp3:VenusPest* in *entpd5a:pkred* expressing larvae revealed that *bmp3* is progressively expressed in sheath cells along the AP axis, ahead of *entpd5a* (Figure 2A, A' and B, B'; Figure S2A). During early stages of notochord segmentation (*i.e.*, in the unsegmented notochord), *bmp3* expression turns on several segments ahead of *entpd5a* (Figure 2A, A' arrows, and Figures S2A), whereas in mature, anterior segments (Figure 2A, A' arrowheads), and at later stages (Figure 2B, B'), the two expression patterns overlap. Together with the *BRE:d2GFP* reporter (Figure 1B–E'), these data indicate that various BMP signaling components are active in the notochord sheath prior to the activation of Notch and *entpd5a*.

To determine whether *bmp3* is required for notochord segmentation, we followed an F0 CRISPR/Cas9 targeting strategy[22] and designed a pool of gRNAs targeting 4 regions of the *bmp3* gene in all three exons (Figure S2B). We chose this approach because BMPs play important roles during early embryo development[23,24] and this helps bypass those early requirements. The pool of gRNAs and Cas9 protein was injected into one-cell stage embryos containing *entpd5a:pkred* and a *TP1:VenusPest*[25] reporter to mark Notch activity. To determine the effects of *bmp3* loss on segment initiation and growth, individual fish were imaged at 10 and 13 dpf. Upon loss of *bmp3*, notochord segmentation was severely impaired, as indicated by both a lack of Notch activation and impaired *entpd5a:pkred* expression (Figure 2C, D). Compared to control siblings of the same developmental stage (standard length[26]), fish injected with the *bmp3* gRNAs had significantly fewer segments at 10 dpf (Figure 2G) and segments were smaller in area along the AP axis (Figure 2H, I). At 13 dpf, larvae showed a decrease in both dorsoventral (DV) and lateral segment growth compared to control siblings (Figure 2D), with some individuals failing to form any *TP1/enptd5a+* segments (Figure S2E, E'). To determine the effect of *bmp3* loss on canonical BMP signaling, we also analyzed *BRE:d2GFP* expression. Interestingly, loss of *bmp3* decreased *BRE:d2GFP* expression (Figure 2E, F), suggesting *bmp3* functions upstream of canonical BMP signaling during sheath cell differentiation. However, the downregulation of *BRE:d2GFP* at the center of mature *entpd5a+* domains in WT (Figure 1E) suggests that high expression of Bmp3 may eventually downregulate Bmp2/4. Together, these data indicate that *bmp3* is essential for notochord segmentation, regulating segment growth in both the DV and AP dimensions.

BMP signaling induces Notch activation in the notochord sheath

The dynamics of BMP activity suggest it functions upstream of Notch during sheath cell differentiation. To test this possibility, we used the QF2/QUAS system[27] to drive the expression of a constitutively active (CA) type I BMP receptor specifically in the

notochord sheath. RNAseq data indicated that *bmpr1ba* is the most abundant of the four type-I BMP receptors expressed in the *col9a2+* domain during segmentation (Figure 1A, S1A). We, therefore, generated a *CAbmpr1ba* DNA construct by introducing a Gln to Asp mutation in the GS domain of *bmpr1ba,* as used previously in other systems[28], and used *p2a-mCherry* to mark expressing cells. The *QUAS:CAbmpr1ba-p2a-mcherry* construct was injected into zygotes containing a stable *col9a2:QF2* transgene[2] to specifically drive expression in *col9a2+* cells. A *QUAS:mcherry-NTR* plasmid was used as a control and *TP1:VenusPest*[25] marked Notch activation in the sheath as shown previously[2]. Mosaic expression of *CAbmpr1ba* in the sheath led to ectopic activation of Notch signaling, as indicated by *TP1:VenusPest* activity (Figure 3B and B'), while overexpression of the control construct did not (Figure 3A and A'). Ectopic Notch activation was detected in 91.6% of cells containing the *CAbmpr1ba* construct prior to notochord segmentation (Figure 3B arrows), as well as in 97.7% of cells at later stages within the IVD domains (Figure 3B' arrows), compared to 10.1% and 8.25% in control fish, respectively.

To test the requirement of *bmpr1ba,* we used the same F0 targeting strategy[22] described above. Pools of gRNAs targeting the GS, ATP binding, and kinase domains of *bmpr1ba* were injected at the single cell-stage along with Cas9 protein (Figure S3A, B). Upon loss of *bmpr1ba*, sheath cell segmentation was delayed and *enptd5a+* segment areas were reduced (Figure 3D, D'). At later developmental stages, lateral growth was also affected, periodically leading to jagged segment boundaries (Figure S3D). However, the effects of *bmpr1ba* loss were mild compared to the phenotype observed when *bmp3* was targeted (Figure 2C–I and S2E, E'). We hypothesized this was due to compensation by other type I BMP receptors in the sheath (Figure 1A, S1A). To address this possibility, we simultaneously knocked down *bmpr1ba* and *bmpr1aa*. When targeted together, the phenotype observed was more severe and segment size was significantly reduced compared to controls (Figure 3E–F').

Next, we investigated the downstream effector Id2a, which demonstrated similar expression dynamics to the *BRE:d2GFP* reporter (Figure 1F, S1B). Similar to *bmpr1ba*, we found that loss of *id2a* leads to delayed segmentation (Figure S3E–F').

Together, these data show that BMP signaling is sufficient to activate Notch in the sheath and suggest BMP acts upstream of Notch during notochord segmentation.

BMP antagonism by Noggin3 limits segment growth

Several antagonists are known to block BMP pathway activation[7,20,29]. Examining our RNAseq data, we found that several *noggin* and *follistatin* genes are expressed in sheath cells (Figure 1A, S1A). Among them, *noggin3* is the most highly upregulated BMP antagonist within the *col9a2+* and double+ domains (Figure S1A). Upon secretion, Noggins directly bind and sequester BMP ligands, thereby preventing the interaction of BMP ligands with their target receptors[20,30]. To monitor *noggin3* dynamics, we generated a promoter knock-in line (*nog3:VenusPest*) using the same strategy described above for *bmp3*[21]. Live confocal imaging over time revealed that *noggin3* expression in the sheath is highly dynamic. Initially, *noggin3* is expressed in regions fated to become mineralizing domains, ahead of *entpd5a* activation (Figure 4A). As notochord segmentation progresses,

the prospective IVD domains turn on *noggin3* in an anterior to posterior fashion, essentially unsegmenting the expression pattern (Figure 4B). At later stages, *noggin3* expression turns off in the *entpd5a+* domain and is highly enriched in *col9a2+* domain and at segment boundaries (Figure 4C).

To assess Noggin3's function in the sheath, we again used the QF2/QUAS system. A *QUAS:nog3-p2a-mcherry* construct was generated and injected into *col9a2:QF2; TP1:VenusPest* transgenic fish at the single cell stage. *QUAS:mcherry-NTR* was injected as a control. Live confocal imaging between 9 and 15 dpf revealed that overexpression of *noggin3* in the notochord sheath strongly diminished Notch activity and caused dramatic notochord segmentation defects compared to control larvae of the same developmental stage (Figure 4D–F). In *noggin3* overexpressing fish, notochord segments were frequently skipped, indicating that the periodicity of segmentation was altered (Figure 4D' asterisks). Moreover, segment area along the AP axis was significantly decreased (Figure 4E), underscoring the importance of BMP signaling during segment expansion. Interestingly, *TP1:VenusPest* expression could still be detected in some cells on the dorsal and ventral sides where segments should have grown (Figure 4D' arrows), which was apparent by plotting the DV extent of *TP1+* segments along the AP axis (Figure 4F). These sites may represent segment seeds formed at notochord-myosepta contacts[31]. Furthermore, the ventral side of some presumed segment initiation sites were often fused with adjacent segments (Figure 4D' arrowhead), suggesting that *noggin3* plays a complex role in regulating boundary formation.

In parallel, we investigated the effects of knocking down *noggin3*. Following the F0 CRISPR strategy described previously[22], we designed and injected 4 gRNAs targeting the *noggin3* gene at the single cell stage (Figure S3G,H). Loss of *noggin3* increased BMP activity along the length of the sheath, as indicated by *BRE:d2GFP* expression (Figure 4G,G'). In sharp contrast to the pooled gRNA experiments performed previously, targeting *noggin3* caused fish to segment slightly faster, averaging roughly two *entpd5a+* segments more than control siblings at 12 dpf. However, the overall effects of *noggin3* loss seemed milder than anticipated. Unlike overexpressing *CAbmpr1ba*, we did not observe ectopic sheath cell differentiation in the IVD domains, except for some instances of anterior segment fusion (Figure 4H'), apparent in a plot of segment area along the AP axis (Figure 4H" arrows). We speculate that the relatively mild phenotype may be due to compensation from other BMP antagonists such as *fstl1b*, *nog2*, and *bmper*, which are also robustly expressed to varying degrees in all three domains (Figure 1A, S1A).

Altogether, our data show that BMP signaling regulates the induction of mineralizing domains upstream of Notch. This may occur via BMP upregulation of *notch1a* and/or *notch2* expression. Our data also suggest that segment initiation and growth are differentially regulated, as illustrated by the continued presence of segment initiation sites when BMP signaling is blocked (Figure 4D'). Based on our functional data and the expression dynamics of the *noggin3* and *bmp3* transcriptional reporters, we propose that Noggin3 functions to prevent premature formation of mineralizing segments and that its inhibitory effect is then overcome as BMP ligand expression builds up along the AP axis. As *entpd5a+* domains

grow laterally, robust expression of Noggin3 in the *col9a2+* domain may limit segment expansion, facilitating the formation of sharp segment boundaries.

Our data suggest that Bmp3 and Noggin3 are components of a differentiation wave in the notochord sheath that travels from anterior to posterior along the AP axis and from the center to the periphery of each notochord segment. The complex landscape of BMP/Notch signaling in the notochord sheath also suggests that other effectors in these pathways and additional spatial cues[31] likely interact to refine the segmentation process. Future studies investigating these pathways may elucidate the mechanism underlying the robustness of notochord segmentation and spine patterning.

STAR Methods

RESOURCE AVAILABILITY

Lead Contact

- Information about resources and reagents used in this study can be directed towards our corresponding author, Michel Bagnat, PhD (michel.bagnat@duke.edu)

Materials availability

- All zebrafish lines and plasmids generated during this study are available upon request without restriction.

Data code availability

- RNAseq Data is originally from Wopat et al, 2018 (GEO: GSE109176). Microscopy data reported in this paper will be shared by the lead contact upon request.
- MATLAB code generated for this study has been deposited on Github and can be viewed at the link listed in the Key Resources Table
- Any additional information required to reanalyze the data reported in this paper is available from the lead contact upon request.

EXPERIMENTAL MODEL AND SUBJECT DETAILS

Zebrafish used in this study were raised and maintained under standard conditions[32] in compliance with internal regulatory review at Duke University School of Medicine. Zebrafish larvae from an Ekkwill (EK) or AB/TL background were used for this study and wild type EK or AB/TL siblings were used as controls for all genetic manipulation experiments. Mutants and transgenic lines used in this study include: *Tg(col9a2:GFPCaaX)*^{pd1151} [2,33], *Tg(col9a2:QF2)*[2], *TgBAC(entpd5a:pkRED)*^{hu7478} [3], *TgKI(nog3:VenusPest)*^{pd1262}, *TgKI(bmp3:VenusPest)*^{pd1267}, *Tg(TP1:VenusPest)*^{s940} [25], *Tg(BRE-AAVmlp:d2GFP)*^{mw30} [11].

METHOD DETAILS

Knockdown of BMP signaling components

Targeting *bmpr1ba*: 5 sgRNAs were pooled together targeting 3 functional domains of the *bmpr1ba* gene. These target sites include the GS domain, ATP binding domain, and kinase domain. A working solution containing 10ng/μL of each sgRNA and 250ng/μL Cas9 protein was injected at the single cell stage into wild type fish containing *col9a2:GFPCaax* and *entpd5a:pkred* transgenes.

The following target sites were used to generate each sgRNA: 5' AGGGAGTCCTGAGCCAGAACCGG 3'; 5' TGGCTCAGGACTCCCTCTACTGg 3'; 5' GAGGACGGTCTGATAGATCTCGG 3'; 5' GATGGTGACACAGATCGGGAAGG 3'; 5' CGCTATGGAGAAGTGTGGATGGG 3'.

bmp3: 4 sgRNAs were generated and pooled as mentioned previously. A working solution containing 10ng/μL of each sgRNA and 250ng/μL Cas9 protein was injected at the single cell stage into wild type fish containing *TP1:VenusPest* and *entpd5a:pkred* transgenes. Guides were designed to target all three exons of the *bmp3 gene.* The following target sites were used: 5' AGCGATCCATGCTGGAGGTGCGG 3'; 5' GGAGCGGGTTCTTGTGTCGTGGG 3'; 5' TGCTCGCAGATATTTAAAGGTGG 3'; 5' CGGGCAGTCGGTGTGGTGCCGGG 3'.

noggin3: 4 sgRNAs were generated and pooled as mentioned previously. A working solution containing 10ng/μL of each sgRNA and 250ng/μL Cas9 protein was injected at the single cell stage into wild type fish containing *BRE:d2GFP* and *entpd5a:pkred* transgenes. Guides were designed to target multiple regions of the *noggin3* coding region. The following target sites were used: 5' GATATCACGGGGTACTGAACGGG 3'; 5' AGAGGACAAGCACGCGGGACAGG 3'; 5' GGAGGACCCGGATCCCGTACTGG 3'; 5' TGTCGCTTGGAATGGGACGGAGG 3'

id2a: Injection solution was made as described above. Several regions of exon 1 were targeted. The following target sites were used: 5' GCCTGCATCACCCGCGAGCGGGG 3'; 5' GCTGAGAGGATCGTCCACGGGGG 3'; 5' CGAGATTCCCTGTTCGCGCTGGG 3'; 5' GATCGCGCTCGACTCCAATTCGG 3'

Generating endogenous promoter knock-in lines: Our strategy for generating endogenous reporters was adapted from a previous study[21]. A donor sequence containing a GFP gRNA target site (*gbait*), the heat shock promoter (*hsp701*), and destabilized Venus (*VenusPest*) was generated in a *puc19* plasmid. The naturally occurring *gbait* site within *VenusPest* was mutated using site directed mutagenesis to yield the following sequence: 5' GGtGAaGGaGAcGCaACtaAtGG 3'. A PCR donor was amplified from the plasmid using the following primers: puc19_F: 5' gttttcccagtcacgacgtt 3'; puc19_R: 5' tgtggaattgtgagcggata 3'. A stock injection solution containing the following was injected at the single cell stage: PCR donor (8ng/μL), Cas9 protein (166ng/μL), *gbait* gRNA (8ng/μL), target site gRNA (16ng/μL), phenol red

The following gRNA target sites were used to generate the endogenous *bmp3* reporter: target_1: 5’ tgggcgcattcggacactattgg 3’; target_2: 5’ GCTGCATGAACGTCGATCTTTGG 3’

The following gRNA targets were used to generate a *noggin3* reporter: target_1: 5’ AGGAGCCCGCGAGCTCACACAGG 3’; target_2: 5’ GGGTTGCATCGCGACCCGCGAGG 3’

Overexpression of a constitutively active BMP receptor: Cut and paste cloning was used to generate the *QUAS:CAbmpr1ba-p2a-mCherry* construct. The vector containing *QUAS:p2a-mCherry* was amplified using the following primers with restriction sites attached: 5’ SphI_p2a_mCherry_F: 5’ CGCGCATGCGACCCAGCTTTCTTGTAC 3’; NheI_QUAS_R: 5’ CGCGCTAGCGGAGCCTGCTTTTTTGTAC 3’. *bmpr1ba* cDNA was amplified using the following primers with NheI and SphI restriction sites attached: NheI_bmpr1ba_F: 5’ cgcGCTAGCTTACAACAACTCGCGGACAC 3’; SphI_bmpr1ba_R: 5’ cgcGCATGCGACTTTAATGTCCTGGGATTC 3’. Both insert and vector were digested with NheI-HF and SphI-HF (NEB) enzymes and ligated together using T4 DNA ligase (NEB).

The *bmpr1ba* sequence was subsequently mutated by site-directed mutagenesis to generate a constitutively active form. The C terminal glutamine within the GS domain was mutated to aspartic acid[28]. The following primer sets were used for this process: CA_bmpr1ba_F: 5’ TATAGCGAAGGACATCCAGATGGTGACAC 3’; CA_bmpr1ba_R: 5’ GTGCGCTGCACCAGTAGA 3’

Overexpression of *noggin3*: To generate a *noggin3* overexpression construct, the *QUAS:bmpr1ba-p2a-mCherry* construct was used as a template. An InFusion (Takara) reaction was performed to swap the *bmpr1ba* sequence for *noggin3* amplified from cDNA. The following primers were used for this process: IF_vector_F: 5’ TACAAAGTGGGGGGATCCGGA 3’; IF_vector_R: 5’ GCTAGCGGAGCCTGCTTT 3’; IF_nog3_F: 5’ GCAGGCTCCGCTAGCGCATTTACGCACCTCGGATAAG 3’; IF_nog3_R: 5’ TCCCCCCACTTTGTAGTTCGGGCAAGAGCATTTG 3’

Microscopy: Live confocal microscopy was performed using an SP8 inverted confocal microscope (Leica) with a 25x/0.95 Fluotar VISIR water immersion objective and Leica Application Suite software (Leica). Fish were anesthetized in 1X tricaine and then mounted onto glass bottom dishes in 1.3% or 0.9% low-melt agarose dissolved in egg water. Egg water was placed on top of the mounted fish to keep fish alive and prevent the agarose and fish from drying out. Digital stitching of tile scans was performed using Leica Application Suite (Leica). Images were false colored and minimally processed for brightness and contrast using ImageJ software (NIH). All images are oriented with the anterior end towards the left.

QUANTIFICATION AND STATISTICAL ANALYSIS

Quantifying *CAbmpr1ba* overexpression—The percent of cells expressing both *CAbmpr1ba* and *TP1* was quantified using the ImageJ point tool to manually count

the number of double positive cells compared to the number of cells solely containing *CAbmpr1ba.* For 9 dpf fish, only the IVD domains or unsegmented regions were quantified. The average percent of double positive cells was reported.

Area and Segment Number Quantification—Image processing and analysis was done in ImageJ and MATLAB. The 8-bit images were pre-processed, first by applying a gaussian blur operation. σ for the function was chosen to be 5 pixels for images containing VenusPest as a fluorescent label and 10 pixels for images containing pKRed. The images were passed with a rolling ball of radius 125 pixels for background subtraction. The notochord was then manually extracted, and the image was segmented using a fixed threshold of 5. After connecting regions of the binary image, a first check identifying the size of the resulting clusters was performed. Any cluster below 50 square pixels was identified as noise and discarded. Any groups close to each other within 80 pixels along the AP axis were also marked as belonging to the same cluster and areas and centroids were merged. The centroids along AP or DV axis were used as a marker of the cluster position. For noggin3 overexpression data, centroid position along the DV axis was rescaled to the local width of the notochord. Any cluster close to the Dorsal or Ventral side (below 0.25 or above 0.75 of the width) was identified as a seed. Area distributions were plotted using the MATLAB addon function CategoricalScatterplot. 1 pixel corresponded to 0.455 μm for these images.

Significance tests for segments and areas were calculated using the Kolmogorav-Smirnov test.

Fluorescence Intensity Profiles—For each pair of fluorescently images marked using pKRed and either VenusPest or GFP, a mask of the entire notochord was first generated manually using the pkRed label and used for both the images. Mean DV intensity values and the standard deviation were plotted along the AP axis.

Supplementary Material

Refer to Web version on PubMed Central for supplementary material.

Acknowledgments

We thank Brian Link for the BMP reporter line and members of the Di Talia and Bagnat labs for discussions. We would also like to thank Krissy Hays for her assistance in normalizing our RNA sequencing data. This work was supported in part by a Faculty Scholars grant from HHMI to M.B. and DST grant from Duke University to S.D.

Inclusion and Diversity

We support inclusive, diverse, and equitable conduct of research.

References

1. Bagnat M, and Gray RS (2020). Development of a straight vertebrate body axis. Development 147. 10.1242/dev.175794.
2. Wopat S, Bagwell J, Sumigray KD, Dickson AL, Huitema LFA, Poss KD, Schulte-Merker S, and Bagnat M (2018). Spine patterning is guided by segmentation of the notochord sheath. Cell Reports 22, 2026–2038. [PubMed: 29466731]

3. Lleras Forero L, Narayanan R, Huitema LF, VanBergen M, Apschner A, Peterson-Maduro J, Logister I, Valentin G, Morelli LG, Oates AC, and Schulte-Merker S (2018). Segmentation of the zebrafish axial skeleton relies on notochord sheath cells and not on the segmentation clock. eLife.
4. Peskin B, Henke K, Cumplido N, Treaster S, Harris MP, Bagnat M, and Arratia G (2020). Notochordal Signals Establish Phylogenetic Identity of the Teleost Spine. Current Biology 30, 2805–2814.e2803. [PubMed: 32559448]
5. Pogoda HM, Riedl-Quinkertz I, Löhr H, Waxman JS, Dale RM, Topczewski J, Schulte-Merker S, and Hammerschmidt M (2018). Direct activation of chordoblasts by retinoic acid is required for segmented centra mineralization during zebrafish spine development. Development 145. 10.1242/dev.159418.
6. Wu M, Chen G, and Li Y-P (2016). TGF-β and BMP signaling in osteoblast, skeletal development, and bone formation, homeostasis and disease. Bone Research 4, 16009. [PubMed: 27563484]
7. Lowery JW, and Rosen V (2018). The BMP pathway and its inhibitors in the skeleton. Physiol Rev 98, 2431–2452. [PubMed: 30156494]
8. Yoon BS, Ovchinnikov DA, Yoshii I, Mishina Y, Behringer RR, and Lyons KM (2005). Bmpr1a and Bmpr1b have overlapping functions and are essential for chondrogenesis in vivo. PNAS 102, 5062–5067. [PubMed: 15781876]
9. Rigueur D, Brugger S, Anbarchian T, Kim JK, Lee Y, and Lyons KM (2015). The Type I BMP Receptor ACVR1/ALK2 is Required for Chondrogenesis During Development. JBMR 30, 733–741.
10. Laue K, Jänicke M, Plaster N, Sonntag C, and Hammerschmidt M (2008). Restriction of retinoic acid activity by Cyp26b1 is required for proper timing and patterning of osteogenesis during zebrafish development. Development 135, 3775–3787. 10.1242/dev.021238. [PubMed: 18927157]
11. Collery RF, and Link BA (2011). Dynamic smad-mediated BMP signaling revealed through transgenic zebrafish. Dev. Dyn 240, 712–722. [PubMed: 21337469]
12. Miyazono K, Maeda S, and Imamura T (2005). BMP receptor signaling: Transcriptional targets, regulation of signals, and signaling cross-talk. Cytokine & Growth Factor Reviews 16, 251–263. [PubMed: 15871923]
13. Uribe RA, Kwon T, Marcotte EM, and Gross JM (2012). Id2a functions to limit Notch pathway activity and thereby influence the transition from proliferation to differentiation of retinoblasts during zebrafish retinogenesis. Dev Biol 371, 280–292. [PubMed: 22981606]
14. Wang H-C, Perry SS, and Sun X-H (2009). Id1 attenuates Notch signaling and impairs T-cell commitment by elevating Deltex1 expression. Mol Cell Biol 29, 4640–4652. [PubMed: 19564409]
15. Daluiski A, Engstrand T, Bahamonde ME, Gamer LW, Agius E, Stevenson SL, Cox K, Rosen V, and Lyons KM (2001). Bone morphogenetic protein-3 is a negative regulator of bone density. Nature Genetics 27, 84–88. 10.1038/83810. [PubMed: 11138004]
16. Gamer LW, Nove J, Levin M, and Rosen V (2005). BMP-3 is a novel inhibitor of both activin and BMP-4 signaling in Xenopus embryos. Dev Biol 285, 156–168. 10.1016/j.ydbio.2005.06.012. [PubMed: 16054124]
17. Banovac I, Grgurevic L, Rumenovic V, Vukicevic S, and Erjavec I (2022). BMP3 Affects Cortical and Trabecular Long Bone Development in Mice. International Journal of Molecular Sciences 23, 785. [PubMed: 35054971]
18. Gamer LW, Cox K, Carlo JM, and Rosen V (2009). Overexpression of BMP3 in the developing skeleton alters endochondral bone formation resulting in spontaneous rib fractures. Developmental Dynamics 238, 2374–2381. [PubMed: 19653325]
19. Komori T (2022). Whole Aspect of Runx2 Functions in Skeletal Development. International Journal of Molecular Sciences 23, 5776. [PubMed: 35628587]
20. Katagiri T, and Watabe T (2016). Bone Morphogenetic Proteins. Cold Spring Harb Perspect Biol 8. 10.1101/cshperspect.a021899.
21. Kimura Y, Hisano Y, Kawahara A, and Higashijima S. i. (2014). Efficient generation of knock-in transgenic zebrafish carrying reporter/ driver genes by CRISPR/Cas9-mediated genome engineering. Scientific Reports 4, 6545. [PubMed: 25293390]
22. Wu RS, Lam II, Clay H, Duong DN, Deo RC, and Coughlin SR (2018). A Rapid Method for Directed Gene Knockout for Screening in G0 Zebrafish. Developmental Cell 46, 112–125.e114. 10.1016/j.devcel.2018.06.003. [PubMed: 29974860]

23. Rogers KW, ElGamacy M, Jordan BM, and Müller P (2020). Optogenetic investigation of BMP target gene expression diversity. eLife 9, e58641. [PubMed: 33174840]
24. Jones WD, and Mullins MC (2022). Chapter Five - Cell signaling pathways controlling an axis organizing center in the zebrafish. In Current Topics in Developmental Biology, Kornberg T, ed. (Academic Press), pp. 149–209.
25. Ninov N, Borius M, and Stainier DY (2012). Different levels of Notch signaling regulate quiescence, renewal and differentiation in pancreatic endocrine progenitors. Development 139, 1557–1567. [PubMed: 22492351]
26. Parichy DM, Elizondo MR, Mills MG, Gordon TN, and Engeszer RE (2009). Normal table of postembryonic zebrafish development: Staging by externally visible anatomy of the living fish. Developmental Dynamics 238, 2975–3015. 10.1002/dvdy.22113. [PubMed: 19891001]
27. Subedi A, Macurak M, Gee ST, Monge E, Goll MG, Potter CJ, Parsons MJ, and Halpern ME (2014). Adoption of the Q transcriptional regulatory system for zebrafish transgenesis. Methods 66, 433–440. [PubMed: 23792917]
28. Wieser R, Wrana JL, and Massagué J (1995). GS domain mutations that constitutively activate TβR-I, the downstream signaling component in the TGF-β receptor complex. The EMBO Journal 14, 2199–2208. [PubMed: 7774578]
29. Correns A, Zimmermann LA, Baldock C, and Sengle G (2021). BMP antagonists in tissue development and disease. Matrix Biol Plus 11, 100071. 10.1016/j.mbplus.2021.100071. [PubMed: 34435185]
30. Brazil DP, Church RH, Surae S, Godson C, and Martin F (2015). BMP signalling: agony and antagony in the family. Trends in Cell Biology 25, 249–264. 10.1016/j.tcb.2014.12.004. [PubMed: 25592806]
31. Wopat S, Adhyapok P, Daga B, Crawford JM, Peskin B, Norman J, Bagwell J, Fogerson SM, Talia SD, Kiehart DP, et al. (2023). Axial segmentation by iterative mechanical signaling. bioRxiv, 2023.2003.2027.534101. 10.1101/2023.03.27.534101.
32. Cunliffe VT (2003). Zebrafish: A Practical Approach. Edited by C. NÜSSLEIN-VOLHARD and R. DAHM. Oxford University Press. 2002. 322 pages. ISBN 0 19 963808 X. Price £40.00 (paperback). ISBN 0 19 963809 8. Price £80.00 (hardback). Genetics Research 82, 79–79. 10.1017/S0016672303216384.
33. Garcia J, Bagwell J, Njaine B, Norman J, Levic DS, Wopat S, Miller SE, Liu X, Locasale JW, Stainier D, and Bagnat M (2017). Sheath cell invasion and trans-differentiation repair mechanical damage caused by loss of caveolae in the zebrafish notochord. Current Biology 27, 1982–1989. [PubMed: 28648824]

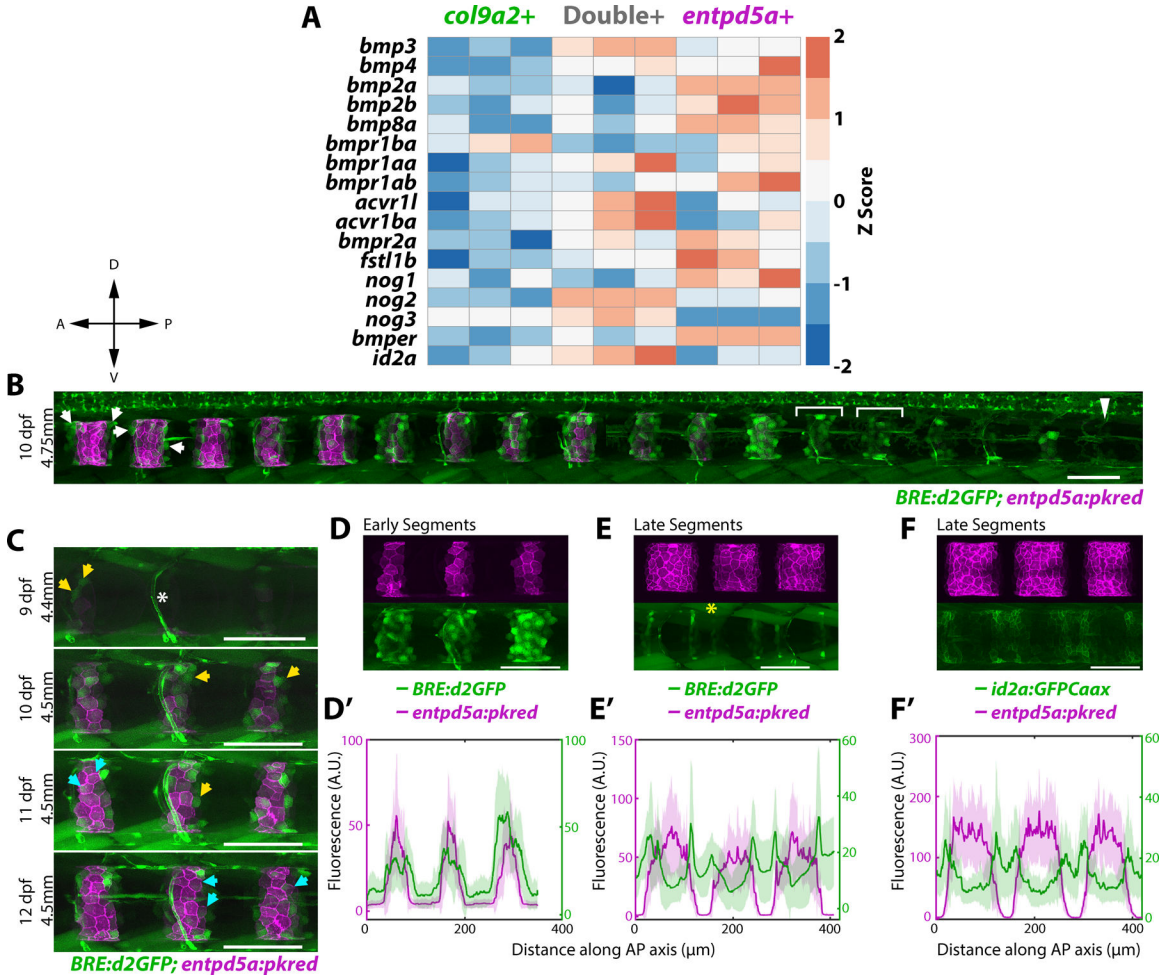

Figure 1: BMP activity is dynamic during notochord segmentation

A) Heatmap of differentially expressed genes in three notochord domains collected from 13 dpf larvae. Primary data is from Wopat et al. 2018. Z-score values were calculated from normalized counts.

B) 10 dpf larva expressing *BRE:d2GFP* and *entpd5a:pkred*. BMP activity is ON at the center of prospective mineralizing domains (brackets) and gets restricted to segment boundaries in mature *entpd5a+* domains (arrows). Arrowhead indicates unsegmented region. n=6 fish. Compass indicates A = anterior, P = posterior, D = dorsal, V = ventral

C) *BRE:d2GFP* and *entpd5a:pkred* expression in the same fish over 4 days. Yellow arrows mark cells that have turned on *BRE:d2GFP*, cyan arrows mark cells that have subsequently decreased *BRE:d2GFP* expression and activated *entpd5a:pkred.* n=3 fish. Asterisk marks blood vessel expression.

D) Newly formed segments expressing both *BRE:d2GFP* and *entpd5a:pkred*. n=6 fish.

D') Fluorescence intensity plot showing overlap of the two expression patterns in (**D**). *BRE:d2GFP* peaks extending more broadly along the AP axis.

E) Mature segments expressing both *BRE:d2GFP* and *entpd5a:pkred* transgenes. *BRE:d2GFP* expression decreased at the center of mineralizing domains and is enriched at segment boundaries. Asterisk denotes muscle expression. n=6 fish.

E') Fluorescence intensity plot of (**E**) showing *BRE:d2GFP* peaks flanking *entpd5a:pkred* expression.

F) Mature segments expressing *entpd5a:pkred* and *id2a:GFPCaax*. n=3 fish.

F') Fluorescence intensity plot of (**F**).

See Figure S1

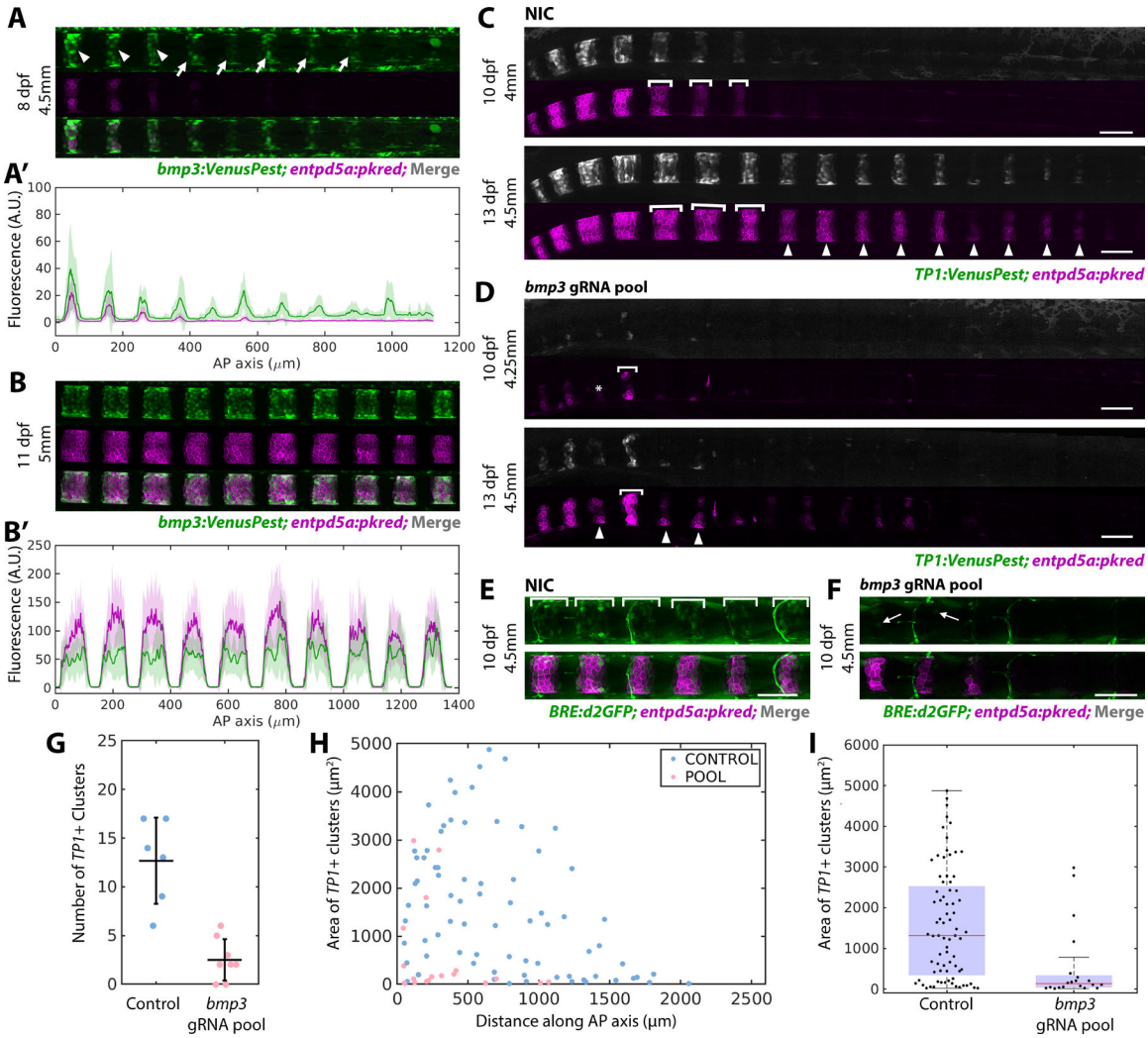

Figure 2: Bmp3 signaling precedes *entpd5a* activation and is required to specify mineralizing cells.

A) *bmp3:VenusPest* expression in the posterior of an 8 dpf larva. Arrowheads mark segments that have activated both *bmp3:VenusPest* and *entpd5a:pkred,* arrows mark *bmp3:VenusPest+* segments without *entpd5a:pkred.* n=3 fish

A') Fluorescence intensity plot of (**A**).

B) Mature segments from an 11 dpf larva expressing *bmp3:VenusPest* and *entpd5a:pkred.* n=4 fish.

B') Fluorescence intensity plot of (**B**) reveals overlapping expression domains.

C) Non-injected control (NIC) larva at 10 and 13 dpf expressing *TP1:VenusPest* and *entpd5a:pkred*. Brackets indicate lateral growth between the two timepoints. Arrowheads mark new segments at 13 dpf.

D) 10 (top) and 13 dpf (bottom) larva injected with *bmp3* gRNA pool. Segments are smaller, irregularly shaped, and fewer in number compared to controls. Asterisk marks a skipped segment, brackets indicate lateral growth between the two timepoints, and arrowheads point to newly formed segments at 13 dpf.

E) WT control 10 dpf larva expressing both *entdp5a:pkred* and *BRE:d2GFP*. Brackets indicate regions of BMP activity. n=6 fish/condition.

F) Larva at the same age and standard length as (**E**) injected with *bmp3* CRISPR pool. Expression of *BRE:d2GFP* and *entpd5a:pkred* are reduced. Arrow indicates cell still expressing *BRE:d2GFP*. n=6 fish.

G) Number of segments at 10 dpf in fish injected with *bmp3* gRNAs compared to controls (horizontal line representing mean ± standard deviation). Data was compiled using MATLAB. Loss of *bmp3* caused a significant decrease in segment number. NIC n = 6, *bmp3* gRNA pools n = 8, p =0.0036.

H) Area of *TP1:VenusPest+* clusters measured along the AP axis in larvae injected with *bmp3* gRNAs and controls at 10 dpf.

I) Distribution of segment areas from (**H**). Loss of *bmp3* leads to decreased segment area along the AP axis. NIC n = 6, *bmp3* gRN*A* pools n = 8, $p = 6.71 \times 10^{-5}$

See Figure S2

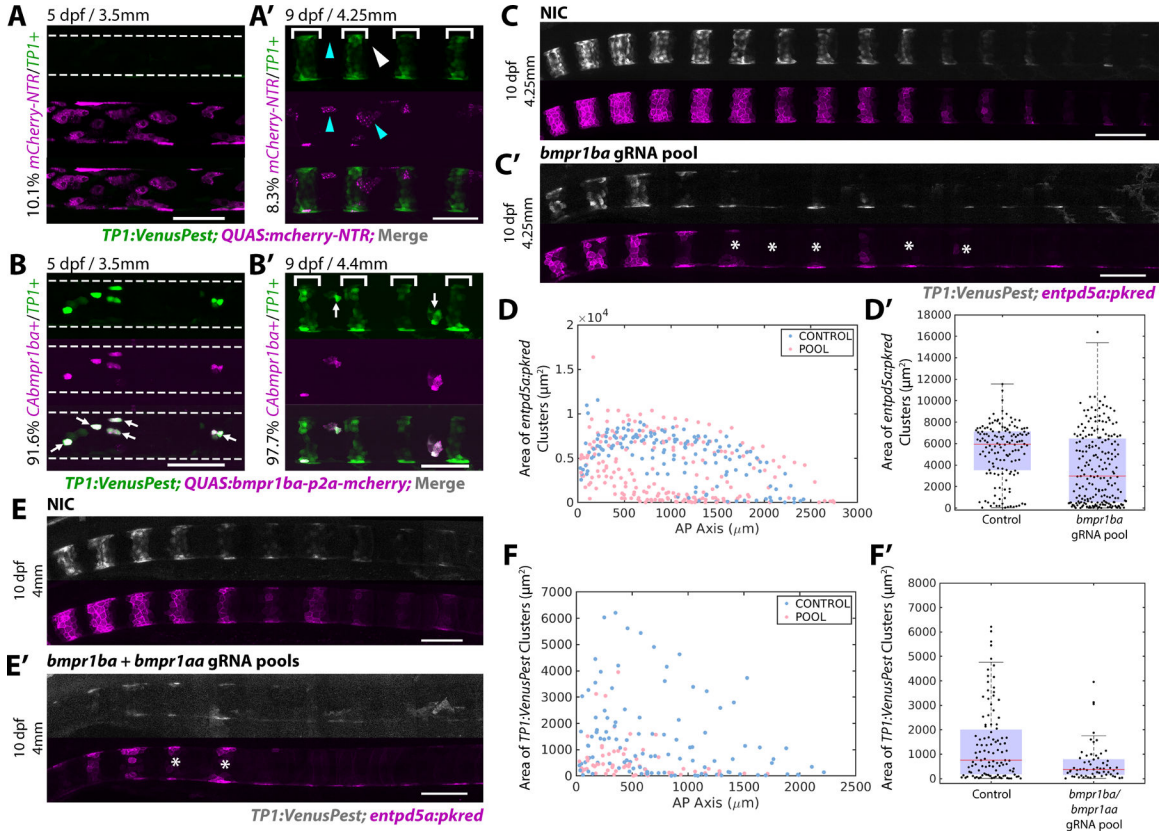

Figure 3: BMP signaling induces Notch activation and establishes mineralizing domains

A, B) 5 dpf larvae injected with either *QUAS:mCherry-NTR* (**A**) or *QUAS:CAbmpr1ba-p2a-mCherry* (**B**) at the single-cell stage. Segmentation has not begun in the region analyzed. Overexpression of *CAbmpr1ba* ectopically activates Notch activity. Overexpression of the control construct does not. An average of 10.1% of cells overexpressing the control construct contained *TP1:VenusPest* expression (n=7 fish, 848 cells). 91.6% of cells overexpressing *CAbmpr1ba* ectopically activated Notch (arrows). (n=6 fish, 630 cells)

A', B') 9 dpf larvae overexpressing the control *QUAS:mCherry-NTR* (**A'**) or *QUAS:CAbmpr1ba-p2a-mCherry* (**B'**) in the sheath. *TP1:VenusPest* is activated in newly formed mineralizing segments (brackets). Of the cells in the IVD domains expressing *QUAS:mCherry-NTR,* 8.25% expressed *TP1:VenusPest* (n=4 fish, 479 cells). Arrowheads indicate cells expressing the control construct that have not activated Notch. *QUAS:CAbmpr1ba-p2a-mCherry* overexpression in the IVD domain caused ectopic Notch activation in 97.6% of cells (arrows). (n=4 fish, 71 cells)

C, C') 10 dpf NIC fish (**C**) and fish injected with a gRNA pool targeting *bmpr1ba* (**C'**). Loss of *bmpr1ba* causes delayed segmentation and incomplete segment growth. Asterisks mark incomplete segments.

D) Segment areas plotted along the AP axis at 12 dpf. Loss of *bmpr1ba* decreased segment area compared to controls.

D') Distribution of segment areas in NIC and *bmpr1ba* gRNA injected fish at 12 dpf . Loss of *bmpr1ba* decreased segment size at this stage, indicating disrupted sheath cell differentiation. (NIC n = 8 fish; *bmpr1ba* gRNA pool n = 12 fish; p value = 1.7945e-08).

E, E') 10 dpf NIC fish (**E**) and fish injected with *bmpr1ba/bmpr1aa* gRNA pools (**E'**) expressing *TP1:VenusPest* and *entpd5a:pkred* show impaired segmentation. Asterisks mark incomplete segments.

F) Segment areas along the AP axis quantified at 10 dpf. (n=8 per condition)

F') Box and whisker plot demonstrating the distribution of areas calculated in (F). (p value = 3.0413e-04).

See Figure S3A-F'

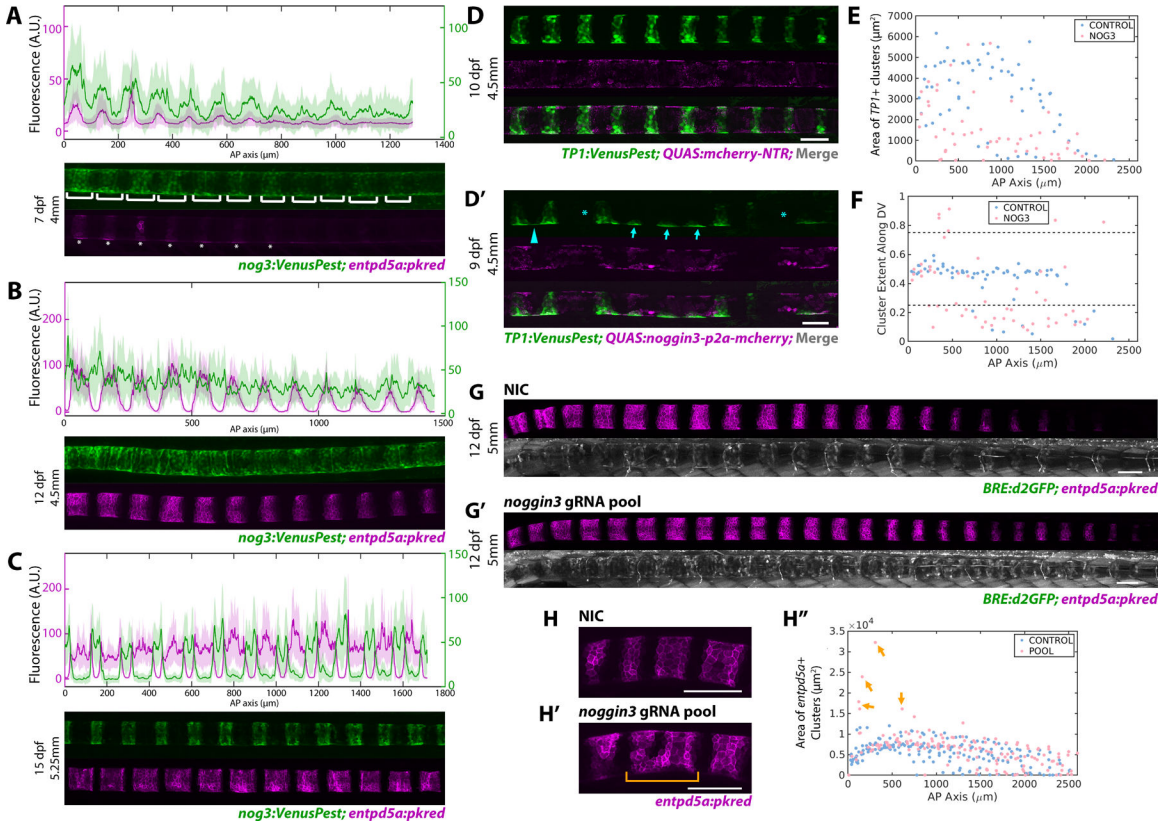

Figure 4: Dynamic expression of the BMP antagonist Noggin3 regulates notochord segmentation

A) *noggin3:VenusPest* expression in the notochord sheath demonstrating expression in the prospective mineralizing domains prior to *enptd5a*. Brackets indicate *noggin3+* segments, asterisks mark segments expressing *entpd5a.* n=4 fish. Florescence intensity analysis (top panel) shows *noggin3:VenusPest* peaking prior to *entpd5a:pkred* with broader expression domains.

B) 12 dpf fish expressing *noggin3:VenusPest* and *entpd5a:pkred*. *entpd5a* expression has expanded laterally as segments begin to mature, *noggin3:VenusPest* expression has begun in the prospective IVD domains, as indicated by the fluorescence intensity plots (top panel). n=3 fish.

C) Later stage (15 dpf) larva depicting mature *entpd5a* segments. *noggin3* has turned off in the mineralizing domains and became restricted to the IVD domains. n=3 fish. Fluorescence intensity plot (top panel) shows *noggin3* enriched at segment boundaries.

D, D') Confocal image of 4.5mm larvae expressing either *QUAS:mCherry-NTR* (**D**) or *QUAS:noggin3-p2a-mcherry* (**D'**) in the sheath. *TP1:VenusPest* shows Notch+ mineralizing segments. Fish overexpressing *noggin3* had skipped segments (asterisks), impaired DV and AP growth (arrows), and ventral fusions (arrowhead).

E) Area of *TP1+* segments is markedly reduced in *noggin3* overexpressing fish compared to controls (n = 4 mCherry control; n = 3 *noggin3*).

F) Plot of cluster centroid locations along the DV axis normalized along the DV width. Control fish develop segments with a ~0.5 DV value, indicating regularly shaped segments with even distribution of *TP1:VenusPest* signal. Fish overexpressing *noggin3* have values

above or below 0.75 and 0.25 respectively, indicating impaired growth in the DV dimension after segment initiation.

G, G') 12 dpf, 5mm fish expressing *BRE:d2GFP* and *entpd5a:pkred.* Fish injected with *noggin3* gRNAs (**G'**) demonstrates an increase in *BRE:d2GFP* expression in the IVD domain and more *entpd5a+* segments compared to controls.

H, H") Loss of *noggin3* caused anterior segment fusions (**H'** bracket), apparent in a segment area plot along the AP axis. (n = 9 NIC; n = 8 *noggin3*)

See Figure S3G,H

KEY RESOURCES TABLE

REAGENT or RESOURCE	SOURCE	IDENTIFIER
Antibodies		
N/A		
Bacterial and virus strains		
N/A		
Biological samples		
N/A		
Chemicals, peptides, and recombinant proteins		
N/A		
Critical commercial assays		
N/A		
Deposited data		
N/A		
Experimental models: Cell lines		
N/A		
Experimental models: Organisms/strains		
Tg(col9a2:GFPCaaX)^{pd1151}	[1,2]	N/A
Tg(col9a2:QF2)^{pd1163}	[2]	N/A
TgBAC(entpd5a:pkRED)^{hu7478}	[3]	N/A
TgKI(nog3:VenusPest)^{pd1262}	This work	N/A
TgKI(bmp3:VenusPest)^{pd1267}	This work	N/A
Tg(TP1:VenusPest)^{s940}	[4]	N/A
Tg(BRE-AAVmlp:d2GFP)^{mw30}	[5]	N/A
Oligonucleotides		
QUAS:CAbmpr1ba-p2a-mCherry	This work	N/A
QUAS:noggin3-p2a-mCherry	This work	N/A
QUAS:mCherry-NTR	This work	N/A
Recombinant DNA		
bmp3 sgRNAs:	This work	N/A
5’ GGAGCGGGTTCTTGTGTCGTGGG 3’		
5’ TGCTCGCAGATATTTAAAGGTGG 3’		
5’ CGGGCAGTCGGTGTGGTGCCGGG 3’		
5’ AGCGATCCATGCTGGAGGTGCGG		
bmpr1ba sgRNAs:	This work	N/A
5’ AGGGAGTCCTGAGCCAGAACCGG 3’		
5’ TGGCTCAGGACTCCCTCTACTGg 3’		
5’ GAGGACGGTCTGATAGATCTCGG 3’		
5’ GATGGTGACACAGATCGGGAAGG 3’		

REAGENT or RESOURCE	SOURCE	IDENTIFIER
5’ CGCTATGGAGAAGTGTGGATGGG 3’		
bmpr1aa sgRNAs:	This work	N/A
5’ AGGTCTGAGACTGGTTGATGAGG 3’		
5’ GAAGGTGTTCTTTACCCGAGAGG 3’		
5’ TGGCCTGTGTCACCTGCATACGG 3’		
5’ GTTCCATCTGTTGGATACGGTGG 3’		
noggin3 sgRNAs:	This work	N/A
5’ GATATCACGGGGTACTGAACGGG 3’		
5’ AGAGGACAAGCACGCGGGACAGG 3’		
5’ GGAGGACCCGGATCCCGTACTGG 3’		
5’ TGTCGCTTGGAATGGGACGGAGG 3’		
id2a sgRNAs:	This Work	N/A
5’ GCCTGCATCACCCGCGAGCGGGG 3’		
5’ GCTGAGAGGATCGTCCACGGGGG 3’		
5’ CGAGATTCCCTGTTCGCGCTGGG 3’		
5’ GATCGCGCTCGACTCCAATTCGG 3’		
Genotyping primers		
bmpr1ba genotyping primers:		
5’ GCAGCGCACTATAGCGAAG 3’		
5’ acctgcaataaggcctttca 3’		
bmp3 genotyping primers:		
5’ CCTACATGGGATGAGGCCAG 3’		
5’ ACGACTTTGGTGAGATAATCCAC 3’		
noggin3 genotyping primers:		
5’ TACCGTATTTCCTGGCCACC 3’		
5’ GCCGTCTTCTGAGCTTCTTG 3’		
Software and algorithms		
ImageJ		https://imagej.nih.gov/ij/
Adobe Photoshop 2021		https://www.adobe.com/creativecloud.html
Adobe Illustrator 2021		https://www.adobe.com/creativecloud.html
MATLAB		https://www.mathworks.com/products/matlab.html
Original Code	This work	https://github.com/padhyapok/notochord_area_plotter